A TWO LOOP OPTIMAL CONTROL OF FLEXIBLE DRIVE TRAIN VARIABLE SPEED WIND POWER SYSTEMS

Iulian MUNTEANU, Antoneta Iuliana BRATCU, Nicolaos Antonio CUTULULIS and Emil CEANGĂ

"Dunărea de Jos" University of Galaţi
Advanced Control Systems Research Center
111, Domnească, 800201-Galaţi, Romania
Phone/Fax: (+40) 236 46 01 82
E-mails: {Iulian.Munteanu, Antoneta.Bratcu, Nicos.Cutululis, Emil.Ceanga}@ugal.ro

Abstract: This paper presents a two loop optimal control structure for variable speed fixed pitch horizontal axis wind turbines (HAWT) having flexible drive trains. That structure, formed by a low frequency loop and a high frequency loop, is the result of the frequency separation principle adopted in the wind modelling. The optimality of the whole system is expressed by the trade-off between the energy conversion maximization and the minimization of the total load excitation that induces the drive train's mechanical stress. This optimal problem is treated within a complete linear quadratic stochastic approach, whose effectiveness was proved by numerical simulation.

Keywords: power generation, windmills, linearization, optimal control, linear quadratic regulators, performance indices

1. INTRODUCTION

The control problem associated with the wind energy conversion systems consists essentially in optimizing the energy conversion. In the case of fixed pitch horizontal axis wind turbines (HAWT), this is equivalent with maximizing the aerodynamic efficiency described by the power coefficient, C_p.

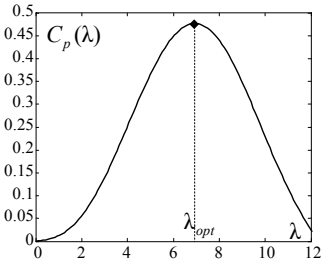

Fig. 1. The power coefficient vs. the tip speed ratio

This coefficient is a function of the tip speed ratio, λ (figure 1), which is defined as a ratio between the peripheral speed of the blades and the wind speed, v:

$$\lambda = \Omega \cdot R / v \,, \tag{1}$$

where Ω is the rotational speed of the blades and R is the blade length. The optimal value of this coefficient being obtained for a well-determined tip speed ratio, λ_{opt} (figure 1), the maximization of the energetic efficiency was implemented in some approaches (e.g., Miller, *et al*., 1997) by controlling the electrical generator in order to track the desired value of the shaft speed, $\Omega^{ref} = v \cdot \lambda_{opt} / R$. This is equivalent to maintaining the operating point on the so called optimal regimes characteristic (ORC) (Nichita, 1995). But this kind of control can induce mechanical reliability problems.

The mechanical fatigue of the drive train can be reduced by imposing the minimization of the generator torque variations, $\Delta\Gamma_G(t)$. Ekelund (1997)

has expressed the antagonist demands of maximizing the energy conversion and minimizing the torque variations by a combined optimization criterion:

$$I = E\left\{\alpha \cdot \left(\lambda(t) - \lambda_{opt}\right)^2\right\} + E\left\{\Delta\Gamma_G^2(t)\right\}, \qquad (2)$$

where $E\{\cdot\}$ is the statistical average symbol. The positive coefficient α is introduced to adjust the trade-off between the two demands above mentioned. The resulted LQG optimization problem has been solved using an adaptive control structure. Munteanu, *et al.*, (2003) developed a new optimal control structure, minimizing the combined criterion (2) with no use of adaptive structures. Its basic principle relies upon separating the turbulence and the seasonal (low frequency) wind speed components from the wind spectral models (Nichita, *et al.*, 2002). In this paper the same structure is used, but for a flexible drive train based HAWT, associated with another form of the optimization criterion. Moreover, a prediction method is used to estimate the seasonal wind speed, instead of filtering it from the total wind.

The paper is organized as follows. In the next section the modelling issues that justify the proposed two loop control structure are presented; this structure is detailed in section 3, as composed of a low frequency loop and a high frequency loop. These loops are designed in sections 4 and 5 respectively. Some simulation results are discussed in section 6 and section 7 is dedicated to the concluding remarks.

2. JUSTIFICATION OF THE TWO LOOP CONTROL STRUCTURE

2.1 Wind modelling

The modelling of the wind power system (WPS) takes into account the wind speed model, using *the frequency separation principle*. The wind speed is modelled as a stochastic process with two components (Nichita, *et al.*, 2002): the seasonal, slowly variable component, $\bar{v}$, and the turbulence, rapidly variable component, $\Delta v(t)$, as identified on the wind model of Van der Hoven (figure 2):

$$v(t) = \bar{v} + \Delta v(t)$$

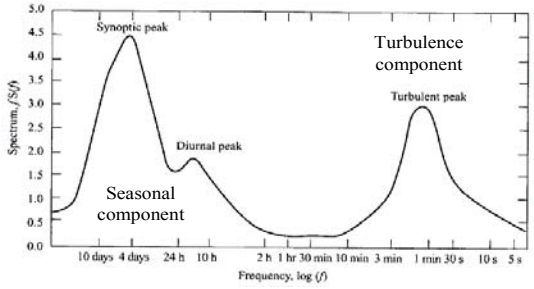

Fig. 2. Large band (six decades) Van der Hoven wind model (Burton, *et al.*, 2001)

The spectral gap around 0.5 mHz (figure 2), meaning negligible wind spectrum energy in the region between 2 hours and 10 minutes, allows the turbulence component, $\Delta v(t)$, be modelled as a zero mean random process. This component is obtained as the output of a first order low-pass (shaping) filter driven by a zero mean white noise, $e(t)$.

It is the low frequency component, $\bar{v}$, that establishes the average position of the operating point on the wind turbine characteristic (the static operating point), whereas $\Delta v(t)$ generates the high frequency variations around this point. Two kinds of dynamics of the WPS may thus be identified: a *low frequency* one, excited by the seasonal component, $\bar{v}$, and described by a steady-state *nonlinear* model, and a *high frequency* one, driven by the turbulence, $\Delta v(t)$, described by a *linearized* model in normalized variations around the static operating point.

2.2 The WPS model

To model a variable speed WPS means essentially to describe the interaction (figure 3) between the aerodynamic subsystem (the rotor of the wind turbine – subsystem S_1) and the electromechanical subsystem, EMS (the asynchronous machine and the static converter – subsystem S_2), through the drive train (subsystem S_3).

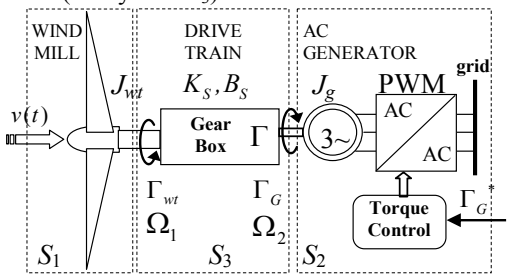

Fig. 3. The structure of the considered WPS

The aerodynamic subsystem is modelled by the nonlinear wind torque characteristic (Wilkie, *et al.*, 1990):

$$\Gamma_{wt} = 0.5 \cdot \pi \cdot \rho \cdot R^2 \cdot v^3 \cdot C_p(\lambda)/\Omega_1 = \Gamma_{wt}(\Omega_1, v), \qquad (3)$$

where ρ is the air density, Ω_1 is the rotational speed of the low-speed shaft and $C_p(\lambda)$ is a polynomial of the tip speed (Nichita, 1995). The asynchronous machine is torque controlled by a vector control scheme, producing the generator torque, $\Gamma_G(t)$, in response to a reference, $\Gamma_G^*(t)$. The dynamics of the EMS can be approximated by those of a first order filter having a time constant, which is negligible versus that of the drive train; therefore $\Gamma_G(t)$ equals $\Gamma_G^*(t)$. The electromagnetic torque reference results from the combined action of the two control loops, as shown in the next section.

The mechanical stress induced by the wind turbulences is usually alleviated if the turbine rotor interacts with the EMS through an elastic coupling based drive train (figure 4). Differently from the rigid

coupling, the two parts of the high-speed shaft, ax*B* and ax*C* in figure 4, are now turning at different speeds, $n\cdot\Omega_1$ and Ω_2 respectively, where n is the transmission ratio of the gearbox. The elastic energy variations yield a new state variable, the internal torque, Γ. Denoting by J_g ax*C*'s inertia and by J_B ax*B*'s inertia, it holds that:

$$J_B = \eta / n^2 \cdot J_{wt},$$

where η is the transmission efficiency and J_{wt} is the low-speed shaft inertia.

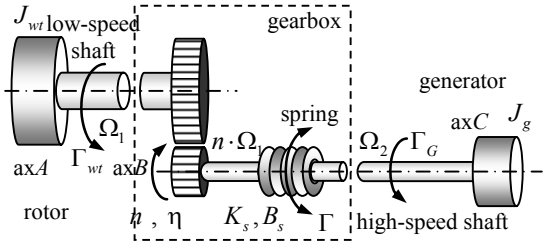

Fig. 4. Flexible drive train

The flexible drive train's model is composed of the ax*B* and ax*C* movement equations and the dynamic of the internal torque (De Battista and Mantz, 1998):

$$\begin{cases} \dot{\Omega}_1 = 1/J_{wt}\cdot\Gamma_{wt} - n/\left(J_{wt}\cdot\eta\right)\cdot\Gamma \\ \dot{\Omega}_2 = 1/J_g\cdot\Gamma - 1/J_g\cdot\Gamma_G \\ \dot{\Gamma} = K_s\cdot\left(n\cdot\Omega_1 - \Omega_2\right) + B_s\cdot\left(n\cdot\dot{\Omega}_1 - \dot{\Omega}_2\right) \end{cases}, \quad (4)$$

where K_s and B_s are respectively the stiffness and the damping coefficients of the spring.

2.3 The linearized model

In the sequel, for a generic variable y of the model, the following notations are adopted:

$$\overline{y} = y\big|_{\text{operating point}} \;;\; \Delta y = y - \overline{y} \;;\; \overline{\Delta y} = \Delta y / \overline{y} \quad (5)$$

Being defined in a *static* operating point, $\overline{y}$ is called *steady-state* value. The nonlinear characteristic of the turbine (3) is linearized around such an operating point, yielding (Ekelund, 1997):

$$\overline{\Delta\Gamma_{wt}} = \gamma\cdot\overline{\Delta\Omega_1} + \left(2-\gamma\right)\cdot\overline{\Delta v}, \quad (6)$$

where γ depends on the chosen operating point:

$$\gamma = \gamma(\overline{\lambda}) = \frac{\overline{\lambda}\cdot \mathrm{d}C_p(\overline{\lambda}) / \mathrm{d}\overline{\lambda} - C_p(\overline{\lambda})}{C_p(\overline{\lambda})}, \quad (7)$$

As the turbulence component results from low-pass filtering a white noise, $e(t)$, its linearized model is:

$$\dot{\overline{\Delta v}}(t) = -1/T_w\cdot\overline{\Delta v}(t) + 1/T_w\cdot e(t), \quad (8)$$

where T_w is the time constant of the shaping filter. The generator torque, Γ_G, acts as the control input in relations (4), which are linearized too. If $\mathbf{x}(t) = \left[\dot{\overline{\Delta\Omega_1}} \;\; \dot{\overline{\Delta\Omega_2}} \;\; \dot{\overline{\Delta\Gamma}} \;\; \dot{\overline{\Delta\Gamma_{wt}}}\right]^T$ is the state vector, $u(t) = \overline{\Delta\Gamma_G}$ is the control input and the normalized variation of the tip speed ratio, $z(t) = \overline{\Delta\lambda}(t)$, is the output (measure) variable, relation (6) and relations (4) linearized lead to the state space matrix equation:

$$\begin{cases} \dot{\mathbf{x}}(t) = \mathbf{A}\cdot\mathbf{x}(t) + \mathbf{B}\cdot u(t) + \mathbf{L}\cdot e(t) \\ z(t) = \mathbf{C}\cdot\mathbf{x}(t) \end{cases}, \quad (9)$$

with:

$$\mathbf{A} = \begin{bmatrix} 0 & 0 & -1/J_T & 1/J_T \\ 0 & 0 & 1/J_G & 0 \\ K_A & -K_A & -B_S\left(1/J_B + 1/J_g\right) & B_S/J_B \\ \gamma/T_w & 0 & -\gamma/J_T & \gamma/J_T - 1/T_w \end{bmatrix},$$
$$\mathbf{B} = \begin{bmatrix} 0 & -1/J_G & B_S/J_g & 0 \end{bmatrix}^T,$$
$$\mathbf{L} = \begin{bmatrix} 0 & 0 & 0 & \left(2-\gamma\right)/T_w \end{bmatrix}^T,$$
$$\mathbf{C} = \begin{bmatrix} 2/\left(2-\gamma\right) & 0 & 0 & -1/\left(2-\gamma\right) \end{bmatrix}, \quad (10)$$

where $J_T = \overline{\Omega_1}\cdot J_{wt}/\overline{\Gamma_{wt}}$ and $J_G = \overline{\Omega_1}\cdot n^2 J_g/\overline{\Gamma_{wt}}$ are time constants, whereas $K_A = \overline{\Omega_1}\cdot K_s n^2/\overline{\Gamma_{wt}}$ is the inverse of a time constant. Note that J_T, J_G and K_A depend on the static operating point, ($\overline{\Omega_1}$, $\overline{\Gamma_{wt}}$). Relations (9) and (10) represent the linearized model of the WPS, describing the dynamics of high frequency variations around the static operating point, impressed by the turbulence component of the wind speed, $\Delta v(t)$. The parameters of the model are depending on this point, so the linearized model of the wind turbine depends on the wind speed.

3. THE PROPOSED CONTROL STRUCTURE

The proposed modelling approach leads to the separate compensation of the two dynamics of the WPS, by means of a two loop control structure.

Due to the high inertia of the turbine versus the wind speed variation, an exclusively based on the energetic optimization control generates large torque variations at the generator's shaft, which are harmful for the mechanical subsystems (the gear-box for example). The global goal of the control aims at achieving a trade-off between the energetic efficiency and reliability, by means of a combined control action obtained in a two loop structure: a *low frequency loop* (LFL), driven by the seasonal wind speed, $\overline{v}$, and a *high frequency loop* (HFL), driven by the turbulence, $\Delta v(t)$. As the maximum energetic efficiency is obtained for a well defined value of the tip speed ratio, λ_{opt}, in the proposed approach the control goal is achieved as follows:

- the steady-state tip speed is maintained at its optimal value, $\overline{\lambda} = \lambda_{opt}$, which describes the

maximum energetic efficiency; this goal is achieved by the LFL, using a classical PI controller for tracking the corresponding rotational speed, $\overline{\Omega_1}$;

- the variations of the tip speed around its mean value are minimized while maintaining the mechanical stress level at reasonable values; this behaviour is optimized in the HFL, using a LQG controller.

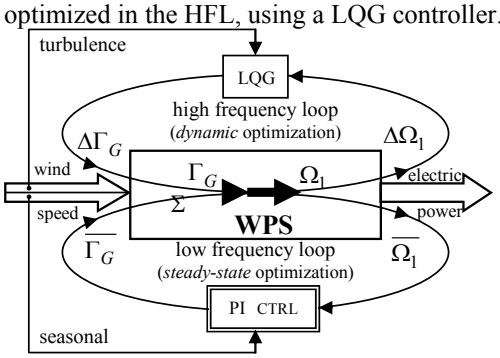

Fig. 5. The proposed control structure

The two components of the wind speed are separated by filtering and they act separately within the two loops of the proposed control structure (figure 5). The same figure shows that the *total* control law is the sum of the two control inputs of the two loops:

$$\Gamma_G = \overline{\Gamma_G} + \Delta\Gamma_G \qquad (11)$$

4. STEADY-STATE OPTIMIZATION: THE LFL

The control problem associated with the LFL concerns the *steady-state* optimization, which consists in operating a wind turbine at variable speed such that its static operating point remains on the ORC. It is proposed that this goal be achieved by tracking the rotor's speed corresponding to λ_{opt}:

$$\overline{\Omega_1}^{ref} = \lambda_{opt} / R \cdot \bar{v} \qquad (12)$$

The LFL (figure 6) generates the static component of the electromagnetic torque, $\overline{\Gamma_G}$ (applied to the high speed shaft), necessary to drive the operating point of the low speed shaft on the ORC.

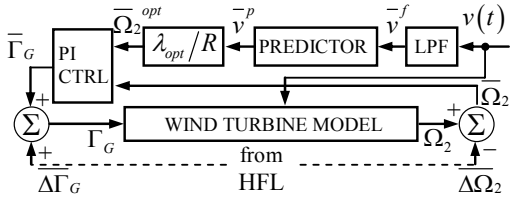

Fig. 6. Low frequency loop

In relation (12) it is the seasonal component of the wind speed, $\bar{v}$, that occurs, as this one determines the (slow) variation of the operating point. In principle, this component can be extracted from the (total) wind speed, $v(t)$, by a high order low-pass filter, whose cut-off frequency must be at most the turbine's bandwidth. But this solution cannot be used in practice without experiencing stability problems due to large phase lags, no matter the chosen control method is. It could happen that the reference torque level be significantly higher than the wind torque, thus compromising the operation of the wind turbine. Different ways have been adopted in order to avoid this problem: to increase the cut-off frequency of the low-pass filter, then making use of the filtering properties of a classical PI controller (Munteanu, *et al.*, 2003), or implementing an on-off controller to zeroing the difference $\bar{\lambda} - \lambda_{opt}$ (Munteanu, *et al.*, 2004). In the present paper, a more accurate estimation of $\bar{v}$ is obtained by combining a reduced order low-pass filtering (LPF) of the total wind with an ARMA model based prediction.

Figure 7 shows the superiority of the presented method versus simple low-pass filtering. Let $\bar{v}^f$ be the output of the LPF and $\bar{v}^p$ the estimation of $\bar{v}$ by filtering and prediction. The speed references computed using either $\bar{v}^f$ or $\bar{v}^p$ in relation (12) will make the system turn at two tip speed ratios, $\bar{\lambda}^f$ and $\bar{\lambda}^p$, as the turbine experiences the real seasonal wind speed, $\bar{v}$. For example, at time 9800 $\bar{v}$ is much less than $\bar{v}^f$; a reference computed using $\bar{v}^f$ would be difficult to track, because the real power available is much below. Meanwhile, the predicted value, $\bar{v}^p$, is closer to $\bar{v}$. One can compare the following standard deviations: $\sigma(\bar{\lambda}^f - \lambda_{opt}) = 0.72$, $\sigma(\bar{\lambda}^p - \lambda_{opt}) = 0.44$.

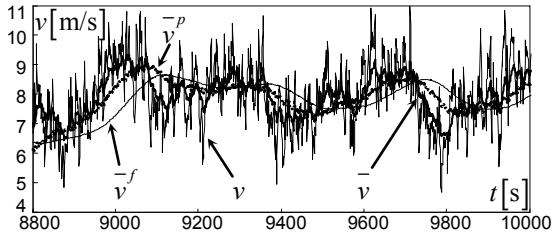

Fig. 7. Predicted versus filtered seasonal wind speed

The ARMA model is recursively implemented for the prediction of the *k*-th sample of $\bar{v}^p$ from $\bar{v}^f$:

$$\bar{v}^p_k = \sum_{i=1}^{n} a_i \cdot \bar{v}^f_{k-i} + \sum_{j=1}^{m} b_j \cdot \left(\bar{v}^p_{k-j} - \bar{v}^f_{k-j} \right) \qquad (13)$$

where m=3, n=6 and a_i, b_j result from a recursive least mean squares procedure (Levine, 1996).

The LFL is based upon a PI controller, as to the Ziegler-Nichols empirical method (Hautier and Caron, 1997), to compensate the (weak) nonlinearities in the neighborhood of an usual operating point. The control practice shows that the PI choice is not critical, even more in the LFL, where the seasonal wind speed varies sufficiently slowly in relation to the wind turbine dynamics. The LFL makes that the mostly variable parameter of the linearized system, γ, be maintained constant with respect to the seasonal wind speed at $\gamma = -1$, and the system (9) be *invariant* in relation to this parameter (Munteanu, *et al.*, 2003).

5. DYNAMIC OPTIMIZATION: THE HFL

5.1 Problem formulation

The most stressed mechanical part of the WPS is the drive train, supporting both the wind torque variations, $\Delta\Gamma_{wt}$, and those of the electromagnetic torque, $\Delta\Gamma_G$. The reliability aspects implying the limitation of the mechanical stress justify the introduction of an optimization criterion expressing a trade–off between the minimization of the tip speed variations around λ_{opt} and the minimization of the total load excitations, that is, $\overline{\Delta\Gamma_{wt}}(t)+\overline{\Delta\Gamma_G}(t)$. This means to track the wind torque variations (Maximization of Energy with wind torque tracking – MEwtt); the optimization criterion (2) becomes:

$$I=\underbrace{E\left\{\alpha\left(\overline{\Delta\lambda}\right)^2\right\}}_{I_1}+\underbrace{E\left\{\left(\overline{\Delta\Gamma_{wt}}(t)+\overline{\Delta\Gamma_G}(t)\right)^2\right\}}_{I_2}\rightarrow\min \tag{14}$$

where the weighting coefficient, α, adjusts the energy-reliability trade-off. The first component results as a quadratic form of the state variable:

$$\begin{aligned} I_1&=E\left\{\alpha\cdot\overline{\Delta\lambda}^2(t)\right\}\rightarrow\min\Leftrightarrow\\ I_1&=E\left\{\mathbf{x}^T(t)\cdot\mathbf{C}_\alpha^T\mathbf{C}_\alpha\cdot\mathbf{x}(t)\right\}\rightarrow\min\end{aligned}, \tag{15}$$

where $\mathbf{C}_\alpha=\sqrt{\alpha}\cdot\mathbf{C}$. The global performance criterion may be put into the form:

$$I=E\left\{\mathbf{x}^T(t)\cdot\underbrace{\left[\left(\mathbf{M}^T\cdot\mathbf{M}\right)+\left(\mathbf{C}_\alpha^T\cdot\mathbf{C}_\alpha\right)\right]}_{\mathbf{R_{xx}}}\cdot\mathbf{x}(t)+2\cdot\mathbf{x}^T(t)\cdot\underbrace{\mathbf{M}^T}_{\mathbf{R_{xu}}}\cdot u(t)+u^T(t)\cdot\mathbf{R_{uu}}\cdot u(t)\right\}\rightarrow\min \tag{16}$$

where $\mathbf{M}$ = [0 0 0 1] and $\mathbf{R_{uu}}$ = 1.

5.2 LQR design

Supposing that the LFL is working, form (16) corresponds to a *linear quadratic invariant stochastic* (Gaussian) optimization problem. The existence and the uniqueness of the problem's solution are guaranteed, as a well-known set of conditions on the structural properties of the controlled system (Levine, 1996) is verified (the justifications are here skipped). The unique optimal control input minimizing the index expressed in (16) for the dynamic system given by relations (9) and (10) is the full-state feedback law, $u(t)=-\mathbf{K}\cdot\mathbf{x}(t)$, with $\mathbf{K}=\mathbf{R}_{\mathbf{uu}}^{-1}\cdot\left(\mathbf{R}_{\mathbf{xu}}^T+\mathbf{B}^T\cdot\mathbf{S}\right)$, where $\mathbf{S}$ is the unique, symmetric and positive semi-defined matrix satisfying the Riccati matrix equation:

$$\mathbf{S}\cdot\mathbf{A}_\mathbf{r}+\mathbf{A}_\mathbf{r}^T\cdot\mathbf{S}+\left(\mathbf{R}_{\mathbf{xx}}-\mathbf{R}_{\mathbf{xu}}\cdot\mathbf{R}_{\mathbf{uu}}^{-1}\cdot\mathbf{R}_{\mathbf{xu}}^T\right)-\mathbf{S}\cdot\mathbf{B}\cdot\mathbf{R}_{\mathbf{uu}}^{-1}\cdot\mathbf{B}^T\cdot\mathbf{S}=0,$$

where $\mathbf{A}_\mathbf{r}=\mathbf{A}-\mathbf{B}\cdot\mathbf{R}_{\mathbf{uu}}^{-1}\cdot\mathbf{R}_{\mathbf{xu}}^T$. The asymptotic stability of the closed loop, described by $\dot{\mathbf{x}}(t)=\left(\mathbf{A}-\mathbf{B}\cdot\mathbf{K}\right)\cdot\mathbf{x}(t)$, is guaranteed.

6. SIMULATION RESULTS

The simulated system is a low power (5.5 kW) high speed fixed pitch HAWT. Its parameters are: R=2.5 m, $\lambda_{opt}=7$, $C_p\left(\lambda_{opt}\right)=0.47$, n=6, J_{wt}=3 kg·m^2, J_g=0.05 kg·m^2, K_s=75 Nm/rad, B_s=0.5 kg·m^2/s.

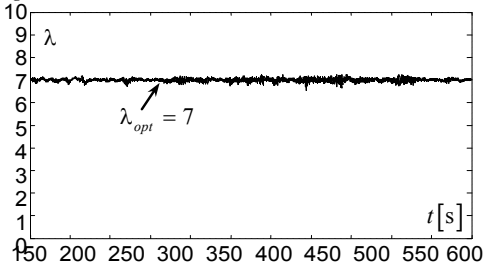

Fig. 8. HFL: the steady-state tip speed ratio kept optimal

Concerning the HFL, any practical implementation of a full-state feedback control requires that all the states be available for measuring. In this case, only the generator's shaft speed, Ω_2, can be directly measured; the other three states need to be estimated. An observer has been computed based upon a pole placement procedure, imposing a time response five times faster than that of the plant (Nise, 2000), and has been used in simulations. Below are briefed some Simulink simulation results on the functioning of each of the two loops and on their combined functioning.

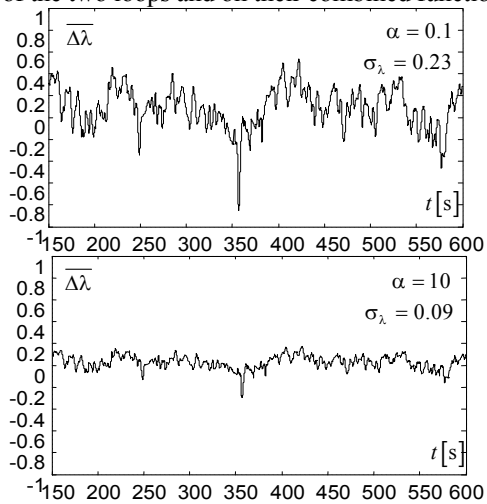

Fig. 9. The evolution of the speed ratio normalized variation for two values of α

Figure 8 presents the LFL functioning: the steady-state value of λ is maintained around its optimal value (in this case λ_{opt}=7). Figures 9 and 10 show how the normalized variations of the tip speed ratio, $\overline{\Delta\lambda}$, and of the sum of torques, $\overline{\Delta\Gamma_{wt}}(t)+\overline{\Delta\Gamma_G}(t)$, depend on α for the same wind sequence. As it was expected, the amplitude of the tip speed normalized variation decreases with α (figure 9), while that of the sum of torques variations increases (figure 10).

One can note that, when α increases from 0.1 to 10, the standard deviation of $\overline{\Delta\lambda}$ decreases from $\sigma_\lambda = 0.23$ to 0.09, while the standard deviation of $\overline{\Delta\Gamma_{wt}}(t) + \overline{\Delta\Gamma_G}(t)$ increases from $\sigma_\Gamma = 0.03$ to 0.53.

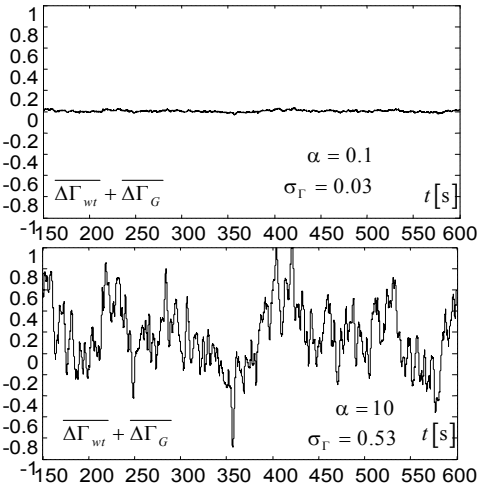

Fig. 10. The evolution of the sum of torques normalized variations for the same two values of α

Figure 11 shows the combined functioning of the two loops, namely the position's variations of the operating point around the ORC for two values of α. One can note that, for small α (top), these variations are significantly larger than those for large α (bottom). Also, it can be noted that these variations increase as the seasonal wind speed increases.

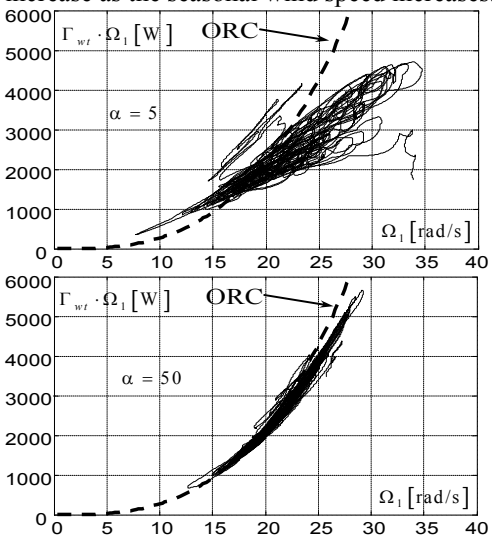

Fig 11. The evolution of the operating point: tracking the ORC

7. CONCLUDING REMARKS

In this paper the synthesis of an optimal control structure for variable speed fixed pitch flexible drive train HAWT is presented. It was used a particular configuration of the control structure – yielded by the frequency separation principle adopted in the wind modelling – consisting of two different loops: the maximum energetic efficiency loop, governed by the low frequency wind speed component, and an optimal control loop, ensuring an energy-reliability trade-off, governed by the turbulence component.

The LFL harvests the maximum energy available in the seasonal wind speed, being built around a PI controller, whose reference is computed using a predicted value of the seasonal wind speed. The HFL is based upon a LQG controller, such that the available turbulence energy is captured more or less, depending on the admissible mechanical stress level. The possibility of variation of the weighting coefficient, α, confers flexibility to the system, so that the wind harvested energy be significantly increased when the particular conditions of the site allow it (that is, when the turbulences are not large).

REFERENCES

De Battista, H. and R. Mantz (1998). Sliding Mode Control of Torque Ripple in Wind Energy Conversion Systems with Slip Power Recovery. In: *Proceedings of the 24th Annual International Conference of the IEEE Industrial Electronics Society (IECON'98)*, August 31–September 4, 1998, Aachen, Germany, pp. 651-656.

Burton, T., D. Sharpe, N. Jenkins and E. Bossanyi (2001). *Wind Energy Handbook*. John Wiley & Sons.

Ekelund, T. (1997). *Modeling and Linear Quadratic Optimal Control of Wind Turbines*. Ph.D. Thesis, Chalmers University of Göteborg, Sweden.

Hautier, J.P. and J.P. Caron (1997). *Systèmes automatiques, tome 2, Commande des processus*. Ellipses, Paris.

Levine, W.S. (Ed.) (1996). *The Control Handbook*. CRC Press.

Miller, A., E. Muljadi and D.S. Zinger (1997). A Variable Speed Wind Turbine Power Control. *IEEE Transactions on Energy Conversion,*. **Volume 12, no. 2**, pp. 451-457.

Munteanu, I., E. Ceangă, N.A. Cutululis and A. Bratcu (2003). Linear quadratic optimization of variable speed wind power systems. In: *Preprints of the IFAC Workshop on Control Applications of Optimization – CAO 2003*, 30 June – July 2 2003, Visegrád, Hungary, pp. 162-167.

Munteanu, I., N.A. Cutululis, A.I. Bratcu and E. Ceangă (2004). Using a nonlinear controller to optimize a variable speed wind power system. In: *Proceedings of the 9th International Conference on Optimization of Electrical an Electronic Equipment* – OPTIM 2004, May 20-23 2004, Braşov, Romania, pp. 303-311.

Nichita, C. (1995). *Étude et développement de structures et lois de commande numériques pour la réalisation d'un simulateur de turbine éolienne de 3 kW*. Thèse de Doctorat, Université du Havre, France.

Nichita, C., D. Luca, B. Dakyo and E. Ceangă (2002). Large Band Simulation of the Wind Speed for Real Time Wind Turbine Simulators. *IEEE Transactions on Energy Conversion*, **Volume 17, no. 4**, pp. 523-529.

Nise, N. (2000). *Control Systems Engineering*. WileyText Books.

Wilkie, J., W.E. Leithead and C. Anderson (1990). Modeling of Wind Turbines by Simple Models. *Wind Engineering*, **4**, pp. 247-274.